International Journal of Modern Physics B, Vol. 16, Nos. 6 & 7 (2002) 1018–1023

CHARACTERISTICS OF CVD DIAMOND FILMS IN DETECTING UV, X-RAY AND ALPHA PARTICLE

J. AHN, B. GAN, Q. ZHANG, RUSLI, S. F. YOON, V. LIGATCHEV, S.-G. WANG, Q.-F. HUANG, K. CHEW

School of Electrical and Electronic Engineering, Nanyang Technological University, Singapore, 639798

A. -C. PATRAN, A.SERBAN, M. -H. LIU, S. LEE

Division of Physics, School of Science, National Institute of Education, Nanyang Technological University, Singapore, 639798

A. A. BETTIOL, T. OSIPOWICZ, F. WATT

Research Center for Nuclear Microscopy, Department of Physics, The National University of Singapore, Singapore, 119260

The CVD diamond UV photodetector shows more than four orders of photoresponsivity discrimination between UV and visible light. Post-treatment on as-fabricated photodetector is essential for a good response to UV light and blindness to visible light. The CVD diamond X-ray detector shows linear dependence of photocurrent on X-ray intensity and high response speed. The mapping of charge collection efficiency on the whole sensing area of a CVD diamond alpha particle detector has been obtained using ion-beam-induced charge microscopy technique. Three peaks have been observed in the charge collection spectrum.

1 Introduction

The wide band gap of CVD diamond makes it a good candidate for UV, X-ray and alpha particle detectors. An ideal diamond UV photodetector is capable of detecting deep UV light and X-rays, but is totally "blind" to visible light. However, non-diamond phase impurities and structural defects in CVD diamond may cause significant photoresponse to visible light. To reduce the extrinsic photoresponsivity to visible light, it is essential to adopt post-treatment on the as-fabricated devices.

The charge collection efficiency of CVD diamond alpha particle detector can be evaluated by the charge collection mapping. The mapping of the charge collection efficiency on the whole sensing area of the detector is important to understand the factors that influence the performance of the alpha particle detectors.

2 Experiment

CVD diamond UV and X-ray photodetectors were fabricated on the growth surface of a 20-μm-thick freestanding diamond film employing coplanar interdigitated metal-semiconductor-metal (MSM) structure and using Ti/Au bi-metal-layer as electrodes. The electrode width and the inter-electrode spacing were kept at 25 μm. After the electrode deposition, the as-fabricated photodetectors were annealed in a nitrogen ambient at 500°C for an hour to make ohmic contacts. At the same time, some photodetectors were

subjected to an O_2 + CF_4 plasma etching at room temperature for half an hour to remove any chemical residue or amorphous carbon on the sensing area between the electrodes.

The photoresponsivity of CVD diamond UV photodetector was measured over a wavelength range of 180~700 nm using a Deuterium lamp (180nm~300nm) and Xe Arc lamp (300nm~700nm). The lamp was dispersed using a ¼ m monochromator with a 1200 grooves/mm grating. A beam splitter with a constant 50:50 splitting ratio in the 180~700nm range were coupled to a sample chamber and a photomultiplier tube. A source/measurement unit (SMU, Keithley 237) was used for the photocurrent measurement.

To investigate the X-ray detector's photoresponse as a function of X-ray intensity, various thicknesses of Aluminum foil was employed to reduce the X-ray intensity in the order of 2. The foil attenuation ratio was calibrated with a Philip XRD machine using its own X-ray flux meter. To evaluate the sensitivity and temporal behavior of a CVD diamond X-ray detector, a pulsed soft X-ray source was employed for the test.

Sandwich structured CVD diamond has been investigated by ion-beam-induced charge (IBIC) imaging technique using a 2 MeV alpha particle beam. The cross-section of a 600-μm-thick diamond films grown by HFCVD was exposed to the alpha particle beam under a bias voltage of 900V. The detector output was connected through a charge preamplifer and a shaping amplifier with a 0.25 μs shaping time to a multichannel analyzer.

3 Results and Discussion

In fabricating the CVD diamond UV photodetectors, post-treatment on the as-fabricated device has been observed to have dramatic influence over the photoresponsivity of the UV photodetectors. It has been reported that a methane-air treatment scheme efficiently increases the photoresponsivity discrimination between the UV and visible light range [1]. In this study, we employed O_2 + CF_4 plasma etching on the as-fabricated photodetectors by reactive ion etching (RIE). The spectral photoresponsivity of a UV photodetector before and after the post-treatment are compared in Fig. 1.

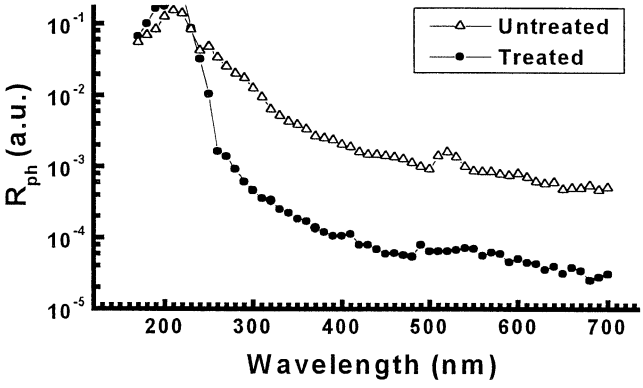

Figure 1. Spectral photoresponsivity of treated and untreated thin-film diamond photodetector.

The photoresponsivity discrimination between UV light (210 nm) and visible light (700 nm) of the CVD diamond detector is found to increase by one order after the O_2 + CF_4 plasma etching as shown in Fig. 1. This could be attributed to the strong etching effect of the plasma on the top surface layer of the sample and reduction of any surface contaminants and amorphous carbon. It is also suggested that the surface plasma etching produces possible defect passivation [2].

In a log-log scale, the photoconductivity of a CVD diamond X-ray detector follows a sublinear power-law dependence on the X-ray flux (F): $\sigma_{ph} \propto F^{\gamma}$. The Rose exponent γ was measured to be 0.668, indicating that some recombination levels are involved in the photoconductivity process of the X-ray detector [3].

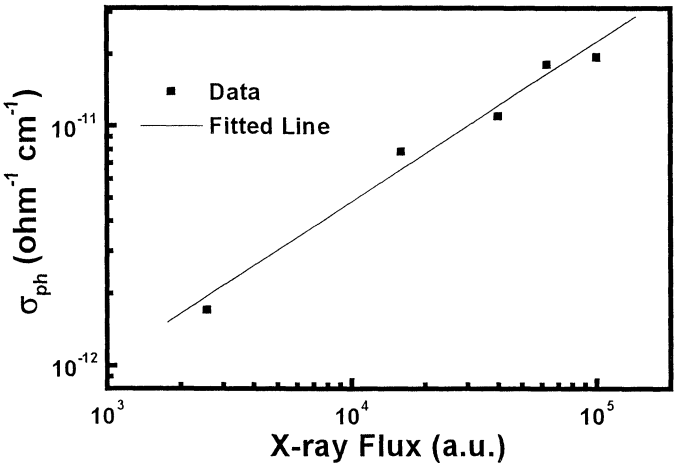

Figure 2. Photoconductivity (σ_{ph}) as a function of X-ray flux (F) under an electric field of 1×10^{4} Vcm^{-1}.

A comparison of the transient photocurrent from diamond thin film (DTF) X-ray detector and the commercial diamond thick film photoconductive detector (PCD), which has a sensing area of 4 x 1 mm^2 and a thickness of 0.5 mm, is shown in Fig. 3. To relate the transient photocurrent of the detector to the X-ray generation system in time, the plasma current derivative dI/dt is also shown.

Previous study has shown that when the plasma focus was working at a low pressure (2.5 mbar), the excited X-ray contains a copious amount of soft X-ray and moderate amount of hard X-ray, which follows the soft X-ray with some time delay [4]. In Fig. 3, two sequential events of soft X-ray and hard X-ray emission have been detected by both DTF and PCD detectors. However, the PCD detector presents very weak signal, more than one order lower than that from DTF detector.

The higher output of the DTF detector to both soft and hard X-ray than the PCD detector may be attributed to the MSM structure, which allows the DTF detector to collect the photon-generated electron-hole pairs efficiently at a high electric field. For PCD detector, although it is superior in film crystal quality, it is practically difficult to obtain high electric field to improve its sensitivity with the electrode gap being 1 mm.

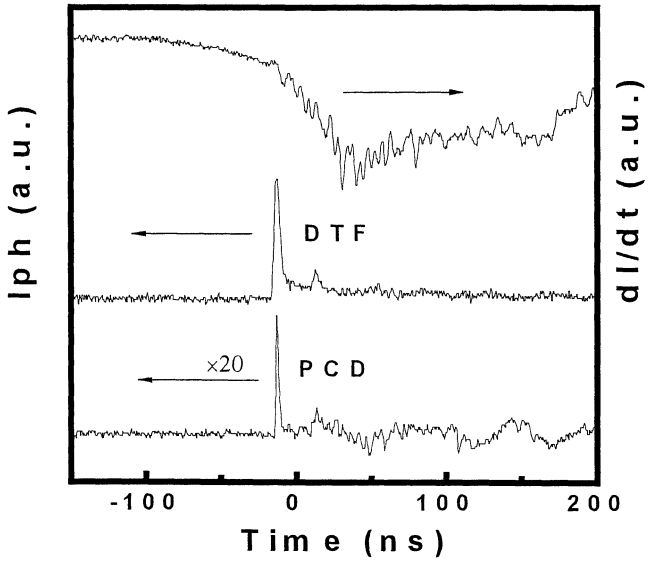

Figure 3. Transient photocurrent excited by soft X-ray of DTF X-ray detector (E= 5 × 10^5 V/cm) and PCD X-ray detector (E = 3 × 10^3 V/cm). They are correlated to the plasma current derivative in time.

Charge collection efficiency is a very important parameter when evaluating a CVD diamond alpha particle detector. In this study, the charge transport distribution on the cross-section of a thick diamond film, which is grown by HFCVD method, has been investigated using a 2 MeV alpha particle source. A bias of 900 V was applied through a pair of sandwich electrodes to a 600-μm-thick film. The substrate side of the film is negatively biased. Reversal of the bias polarity is found to greatly decrease the charge collection efficiency. This is not well understood so far. Figure 4 shows the average charge collection spectrum over the whole mapping area of the cross-section.

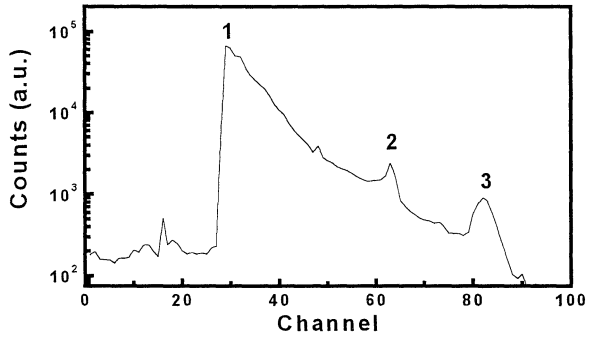

Figure 4. Average charge collection spectrum on the whole cross-section of a 600-μm-thick films from an IBIC microscope. Channal number is proportional to charge collection efficiency.

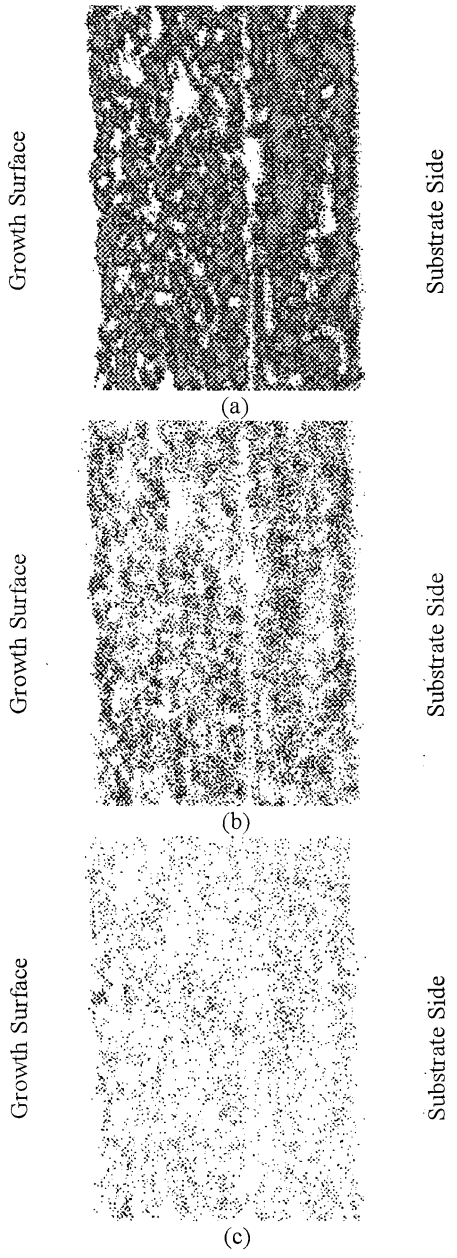

Figure 5. IBIC image of the cross-section acquired using a 2 MeV alpha beam. The size of the image is 1 mm × 1 mm. Three peaks shown in Fig. 4 are respectively shown in Images (a): Peak 1 (Channel 4-50), (b) Peak 2 (Channel 51-72), (c) Peak 3 (Channel 73-93). Dark area corresponds to the location where the charge is collected.

The channel number shown in X-axis is proportional to the charge collection efficiency. The exact value of the charge collection efficiency can be calibrated using a PIN diode, which is able to obtain a charge collection efficiency η of unity. Three peaks are observed above certain threshold of charge collection efficiency. Corresponding to

the three peaks, the IBIC image mapping on the whole area is split into three images, as shown in Figs. 5(a), (b) and (c).

The images in Fig. 5 shows the IBIC distribution obtained under different charge collection efficiency. It can be seen that carrier transport with low charge collection efficiency dominates the whole area, as shown in Fig. 5 (a). Location with higher charge collection efficiency are distributed with lower density, as shown in Fig. 5 (b) and (c). Spatial nonuniformity in the charge collection efficiency from the substrate side to the growth surface can also be seen. This is likely due to the highly nonuniform crystal structure along the cross-section. However, the charge collection efficiency does not show nonuniformity particularly along the film growth direction, as would be expected for the columnar structure. This is partly due to the fact that the film used in our experiment may not preserve good columnar structure, and partly due to the complex distribution of electric field within the films induced by structural defects. Further study is needed to compare the SEM image and IBIC image of the cross-section. It is also necessary for the substrate side to be abraded away to certain thickness so as to decrease the influence of the poor quality grains.

The IBIC images shown in Fig. 5 indicate that the charge collection efficiency η is low (<10%) at an electric field of 1.5×10^4 V/cm. It is reported that CVD diamond always present very low charge collection efficiency η. Even for CVD diamond having by far the highest charge collection distance of 250 μm, the charge collection efficiency η only reaches 20% [5]. This poor detection efficiency is related to the low atomic number and a small cross-section of diamond. In our case, with the substrate side not being polished, the expected advantage of columnar grain in charge transport may be affected by the poor quality of the crystal grain near the substrate side.

4 Conclusion

The characteristics of CVD diamond UV, X-ray and alpha particle detector have been studied. It is demonstrated that an O_2 + CF_4 plasma etching on the as-fabricated photodetectors is helpful to improve the photoresponse discrimination between UV and visible light. CVD diamond thin film X-ray detector presents a sublinear dependence of detector photocurrent on the X-ray photon flux. Under pulsed soft X-ray illumination, the detector shows good sensitivity and short response time. The IBIC image of the cross-section of a CVD diamond thick film alpha particle detector shows that the charge collection efficiency can be further improved by removing the poor quality substrate side.

References

1. M. D. whitfield, R. D. Mckeag, L. Y. S. Pang, S. S. M. Chan, R. B. Jackman, Diamond Relat. Mater., **5**, (1996) pp. 829.
2. O. Gaudin, S. Watson, S. P. Lansley, H. J. Looi, M. D. whitfield, R. B. Jackman, Diamond Relat. Mater. **8**(4), (1999) pp. 886-891.
3. Rose, *Concepts in Photoconductivity and Allied Problems* (Inter-science, New York, 1963).
4. M. Liu, *PhD. Thesis*, NIE/NTU (1996).
5. M. Marinelli, E. Milani, A. Paoletti, A. Tucciarone, G. Verona Rinali, M. Angelone and M. Pillon, Appl. Phys. Letts., **75**(20), 3216(1999).